

# Spin Matching from AGS to RHIC<sup>1</sup>

W. W. MacKay, and N. Tsoupas

*Brookhaven National Laboratory, Upton, NY 11973, USA.*

**Abstract.** With a partial Siberian snake in the AGS and transport lines with interspersed horizontal and vertical bends, the incoming spin direction at the injection points of both the collider rings is not likely to match the ideal vertical stable spin direction of RHIC which has two full helical Siberian snakes per ring. In this paper we examine the matching of a polarized beam transferred from the AGS into RHIC. The present 5% partial solenoidal snake as well as a proposed 20% superconducting helical are considered for the AGS. Solutions with retuned snakes in RHIC to better match the incoming beam have been found.

Ideally in a flat ring without snakes, we should expect the stable spin direction  $\vec{n}_0$  of the closed orbit to be vertical (except at spin resonances). The collider accelerator complex [1][2] at BNL consists of a polarized proton source followed by a linac, the Booster ring, the AGS ring and the two collider rings, not to mention the connecting transport lines. At injection ( $G\gamma = 2.18$ ) and extraction ( $G\gamma = 4.7$ ) in the Booster ring, the stable spin direction is vertical. At present the AGS has a warm solenoidal partial Siberian snake which rotates the stable direction away from the vertical direction. When the partial snake in the AGS is operated with a  $\sim 5\%$  rotation ( $9^\circ$ ), the stable spin direction is tilted  $4.5^\circ$  away from the vertical. Each of the collider rings has a pair of full ( $180^\circ$ -rotation) superconducting helical Siberian snakes to fix the spin tune exactly at 0.5, independent of beam energy. With the snakes the injection points of the collider rings have stable spin directions which are vertical. Injection and extraction in the Booster and AGS rings happen in horizontal plane, but for RHIC we inject vertically.

The AGS is about 1.7 m higher than the RHIC rings, so in the AGS-to-RHIC transfer line (ATR) there are vertical bends interspersed with the normal horizontal bends. Due to the partial snake in the AGS and the vertical bends in the ATR, spin matching from the AGS into RHIC is not perfect. By retuning the RHIC snakes for injection, we can improve the spin transfer from the AGS. In this paper we examine the spin matching from the AGS into RHIC with the present 5% snake and with a proposed stronger superconducting helical 20% snake.

## PRELIMINARIES

First we define our coordinates with positive angles for clockwise bends as in the Blue ring of RHIC as shown in Figure 1. The Pauli matrices for the three directions are defined

---

<sup>1</sup> Work performed under the auspices of the U. S. Department of Energy and RIKEN of Japan.

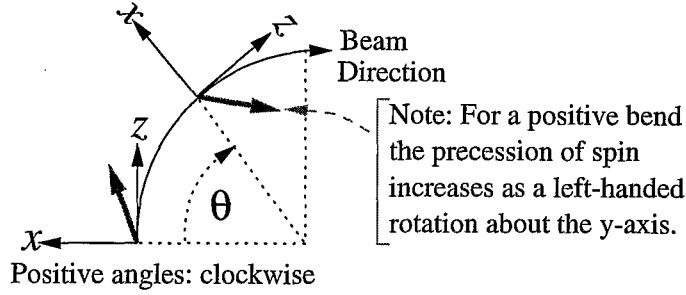


**FIGURE 1.** For the local coordinate system traveling with the beam, the  $z$ -axis points along the direction of the beam,  $y$ -axis points vertically (out of the page), and the  $x$ -axis points to the left thus forming a right-handed system. Clockwise bends (to the right) have a positive bend angle. The projection of the polarization in the horizontal plane is measured relative to the local  $z$ -axis.

as

$$\sigma_x = \begin{pmatrix} 0 & 1 \\ 1 & 0 \end{pmatrix}, \quad \sigma_y = \begin{pmatrix} 0 & -i \\ i & 0 \end{pmatrix}, \quad \text{and} \quad \sigma_z = \begin{pmatrix} 1 & 0 \\ 0 & -1 \end{pmatrix}, \quad (1)$$

so that a left-handed spin rotation about an axis  $\hat{n}$  by an angle  $\theta$  is then given by the  $2 \times 2$  spinor rotation matrix

$$\begin{aligned} \mathbf{R}_{\hat{n}}(\theta) &= e^{i\hat{n} \cdot \vec{\sigma} \theta / 2} = \mathbf{I} \cos \frac{\theta}{2} + i\hat{n} \cdot \vec{\sigma} \sin \frac{\theta}{2} \\ &= \begin{pmatrix} \cos \frac{\theta}{2} + in_z \sin \frac{\theta}{2} & (n_y + in_x) \sin \frac{\theta}{2} \\ (-n_y + in_x) \sin \frac{\theta}{2} & \cos \frac{\theta}{2} - in_z \sin \frac{\theta}{2} \end{pmatrix}. \end{aligned} \quad (2)$$

Note these conventions are different from S. Y. Lee's book[1] and coincide more closely to the usual conventions of quantum mechanics and high energy physics [2]. The defined coordinate systems vary from the Booster (clockwise) to the AGS (counterclockwise) through the ATR (AGS to RHIC transfer line) with a clockwise system to the clockwise Blue ring, and the counterclockwise Yellow ring. (Note that in the Yellow ring the  $s$ -coordinate is defined parallel the Blue ring [3], i.e. opposite to the direction of the beam.) Needless to say things can get very confusing in switching coordinates systems and rotation directions throughout the transport of the beam.

With all this in mind for this paper, we should note that in the AGS and Yellow ring our convention has  $+x$  pointing toward the center of the rings. In the Booster and the Blue ring  $+x$  points away from the center of the rings. With respect to spin rotation this gives:

$$\begin{aligned} \mathbf{R}_x(\pi/2) &\text{ rotating } \hat{z} \text{ into } \hat{y}, \\ \mathbf{R}_y(\pi/2) &\text{ rotating } \hat{z} \text{ into } -\hat{x}, \text{ and} \\ \mathbf{R}_z(\pi/2) &\text{ rotating } \hat{y} \text{ into } \hat{x}. \end{aligned}$$

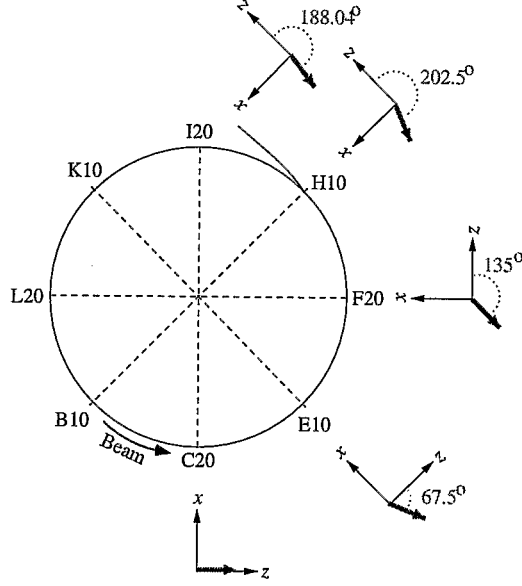


**FIGURE 2.** Basic geometry of the AGS spin precession with a 20% partial snake in the I20 straight section at extraction energy ( $G\gamma = 46.5$ ). For the superconducting helical snake being considered, the snake's rotation axis is longitudinal as in a solenoid.

## AGS EXTRACTION

In the AGS, the beam goes around in the counterclockwise direction as shown in Figure 2. The extraction location is in the H10 straight section, and the new snake will most likely be placed in the I20 straight section. The azimuthal angle from H10 to I20 is

$$-\frac{3}{24} \times 2\pi = -\frac{\pi}{4}, \quad (3)$$

and the angle from the snake back around to H10 is

$$-[2\pi - \frac{\pi}{4}] = -\frac{7\pi}{4}. \quad (4)$$

The corresponding amount of spin precession in these arcs is then

$$\eta_1 = -\frac{\pi G\gamma}{4}, \quad \text{and} \quad \eta_2 = -\frac{7\pi G\gamma}{4}. \quad (5)$$

The beam in the AGS goes around in a counterclockwise direction, so we have the 1-turn spin rotation map

$$\begin{aligned} \mathbf{M} &= \begin{pmatrix} \cos \frac{\eta_2}{2} & \sin \frac{\eta_2}{2} \\ -\sin \frac{\eta_2}{2} & \cos \frac{\eta_2}{2} \end{pmatrix} \begin{pmatrix} \exp(i\frac{\mu}{2}) & 0 \\ 0 & \exp(-i\frac{\mu}{2}) \end{pmatrix} \begin{pmatrix} \cos \frac{\eta_1}{2} & \sin \frac{\eta_1}{2} \\ -\sin \frac{\eta_1}{2} & \cos \frac{\eta_1}{2} \end{pmatrix} \\ &= \mathbf{I} \cos \frac{\mu}{2} \cos \frac{\eta_1 + \eta_2}{2} + i \sin \frac{\mu}{2} \sin \frac{\eta_1 - \eta_2}{2} \sigma_x \\ &\quad + i \cos \frac{\mu}{2} \sin \frac{\eta_1 + \eta_2}{2} \sigma_y + i \sin \frac{\mu}{2} \cos \frac{\eta_1 - \eta_2}{2} \sigma_z. \end{aligned} \quad (6)$$

The fractional tune may be obtained from the trace:

$$2 \cos(\pi\nu) = 2 \cos \frac{\mu}{2} \cos \frac{\eta_1 + \eta_2}{2}. \quad (7)$$

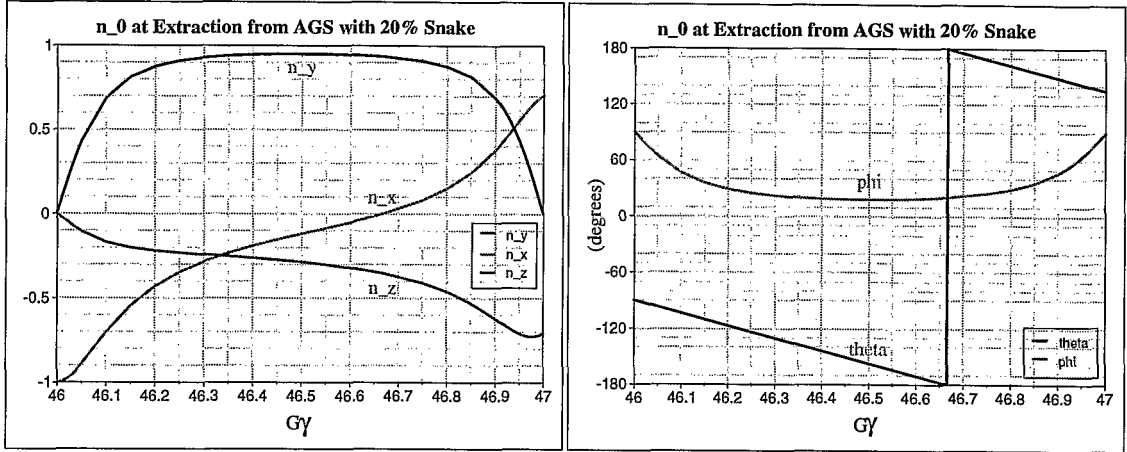


**FIGURE 3.** Plot of  $\vec{n}_0$  at extraction energy at the H10 straight section.  $\theta$  is the angle of the  $\hat{n}_0$  vector away from the vertical, and  $\phi$  is the angle between the z-axis and the projection of the  $\hat{n}_0$  vector on the horizontal plane.

The stable spin direction at the H10 straight section may be easily obtained from Eq. (6):

$$\hat{n}_0 = \frac{1}{\sin(\pi\nu)} \begin{pmatrix} \sin \frac{\mu}{2} \sin \frac{\eta_1 - \eta_2}{2} \\ \cos \frac{\mu}{2} \sin \frac{\eta_1 + \eta_2}{2} \\ \sin \frac{\mu}{2} \cos \frac{\eta_1 - \eta_2}{2} \end{pmatrix}. \quad (8)$$

A plot of  $\hat{n}_0$  versus  $G\gamma$  at H10 shows the dependence on energy of the extraction from the AGS. The vertical spin component is quite stable near the half-integer values of  $G\gamma$ .

## TRANSFER LINE FROM AGS TO RHIC

Due to interleaved horizontal and vertical bends from the AGS extraction to the RHIC injection points, the value of the  $\vec{n}_0$  of the injected beam at the RHIC injection point will vary both with energy and AGS snake setting, and may differ for each of the Blue and Yellow rings. The transfer lines are divided into four sections (See Figure 4a.): first, the U-line with two horizontal bends of  $4.31^\circ$  and  $8^\circ$ ; next, the W-line which provides a horizontal bend of  $20^\circ$  to orient the beam to the switching magnet along a mirror symmetry axis for the RHIC rings; finally the two large arcs the X-line for injection into the clockwise Blue ring and the Y-line for injection into the counterclockwise Yellow ring. Since the planes of the AGS and RHIC rings have a 1.73 m difference in height, there are a pair of vertical bends in the W-line as shown in Figure 4b. The lattice was designed to have a full period of betatron phase advance between the two bends in order to minimize vertical dispersion for injection. Beams are injected into RHIC through vertical septum (Lambertson) magnets. The nominal vertical bends from steering magnets upstream of the septum magnet, two ring quadrupoles downstream of the septum, and the injection kicker magnets (4 modules) are interleaved with horizontal bends as shown in Figure 4c.

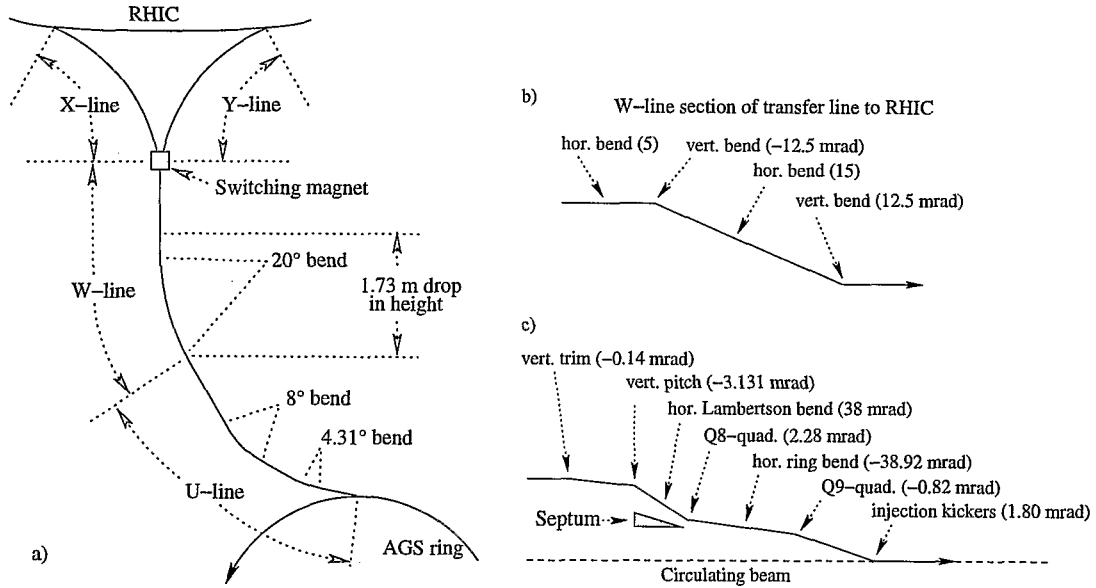


**FIGURE 4.** Layout of the AGS to RHIC transfer lines (ATR). a) Horizontal layout of the ATR. b) Layout of vertical bends for 1.73 m drop to the AGS. c) Vertical layout of injection to RHIC. This figure was drawn for the Yellow ring injection; the horizontal bends of 38 mrad and  $-38.92$  mrad should reverse sign for injection into the Blue ring.

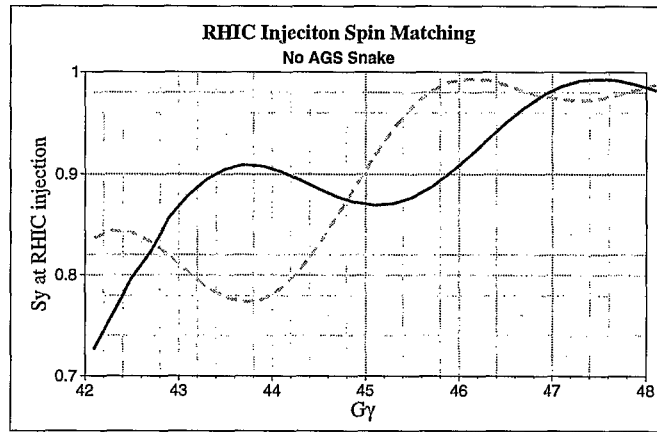


**FIGURE 5.** Spin matching into RHIC with 0% partial snake in the AGS. The solid (dashed) curve shows the matching into the Blue (Yellow) ring for different values of  $G\gamma$ .

Figure 5 shows the vertical projection of the  $\vec{n}_0$  vector at injection into RHIC rings. In the first vertical bend of the W-line,  $\vec{n}_0$  tilts  $\sim 30^\circ$  away from the vertical about the radial axis, then rotates about the vertical by  $G\gamma \times 15^\circ$  in the horizontal bends, and then back by  $\sim -30^\circ$  about the radial axis in the second vertical bend.

When  $\vec{n}_0$  is tilted either forward or backward at the end of the W-line, then we see a mirror symmetric precession through the X and Y-lines. This is shown in Figure 5 for  $G\gamma = 48$  where there is about a net  $10^\circ$  tilt away from vertical in the injection region of Figure 4c.

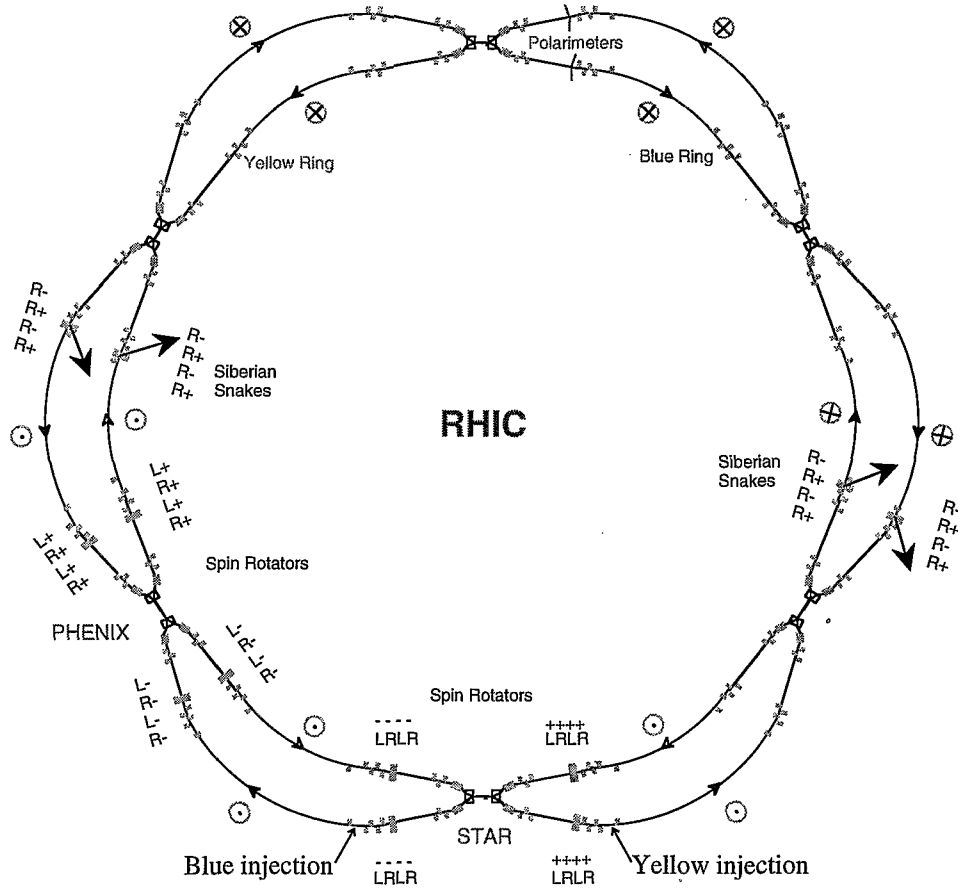


**FIGURE 6.** Layout of RHIC rings. In the Blue ring the beam moves in a clockwise direction, and in the Yellow ring the beam goes counterclockwise. The snakes consist of four right-handed helical dipoles with vertical fields at the ends as indicated (+ for  $\vec{B}_{\text{end}}$  up, - for  $\vec{B}_{\text{end}}$  down). The spin rotators consist of a combination of four right-handed (R) and left-handed (L) helical dipoles with horizontal fields as indicated (- for  $\vec{B}_{\text{end}}$  pointing radially in towards the center of the rings, and + for  $\vec{B}_{\text{end}}$  pointing radially outward from the center of the rings).

## RHIC RINGS WITH TWO SNAKES

Figure 6 shows the placement of polarization equipment in the collider rings. The injection Lambertson magnets are located in the straight sections of dispersion suppressors at the beginning of the lower main arcs on either side of the STAR detector. The two rings are side by side horizontally and cross over at each of the six interaction regions. Two superconducting Siberian snakes (each with four helical dipoles) are located on opposite sides of each ring. There are also four superconducting rotators placed around each of the STAR and PHENIX detectors to rotate the spin locally into the longitudinal direction. A polarimeter is located in each ring just to the right of the north interaction region.

Each RHIC snake consists of four right-handed helical dipoles with a 9.5 cm diameter beam pipe. The snake is powered by two power supplies: one for the end helices in series

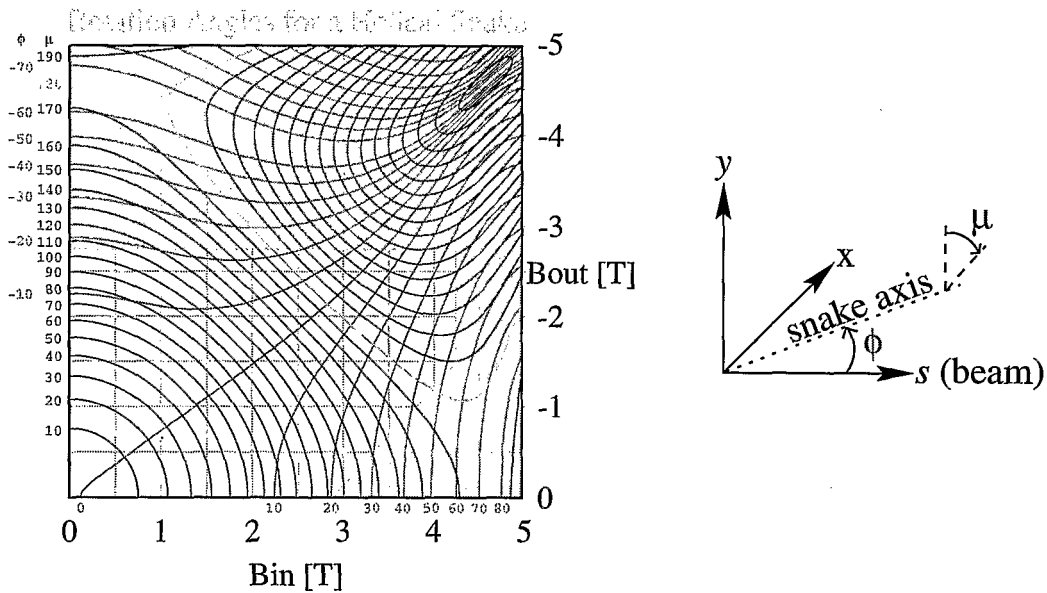


**FIGURE 7.** Field tuning plane for RHIC snakes. The inner pair of helices are powered to the fields  $B_{in}$  and the outer pair to  $B_{out}$ . The darker contours correspond to the rotation angle  $\mu$  and the lighter contours correspond to the angle between the rotation axis and beam's direction. The shaded region corresponds to forbidden regions where the orbit excursion at injection energy reaches the aperture limit, or where the central helices would reach too high a field.

and another for the inner pair of helices also in series. The orbit excursion from one helix is canceled by having the paired helix powered with opposite polarity.

Figure 7 shows the field settings for the two pairs of helices in a given snake to obtain different amounts of rotation of the polarization. With two knobs, there is control of both the amount of rotation  $\mu$  and the direction of the rotation axis  $\phi$ . Although the superconducting helices in the snakes can operate up to 4.2 T, at injection the orbit excursions limit the operating range to the unshaded region of Figure 7. For normal operation the largest orbit excursion is about 3.1 cm vertically in the middle of the snake; this is right at the edge of the shaded contour,  $(B_{in}, B_{out}) = (4 \text{ T}, 1.2 \text{ T})$ . It would be possible to reposition a snake by as much as 1 cm to allow for some modest amount of tuning at injection.

For this study we have kept the snake rotation axes at  $\pm 45^\circ$  in each ring to maintain the spin tune at 0.5. Table 1 shows the injection transfer efficiency to both collider rings with a 20% partial snake located in the I20 straight section of the AGS. Clearly the efficiencies are better if the partial snake field is antiparallel to the beam ( $-20\%$ ). The first two rows show efficiencies with nominal settings for the RHIC snakes, and the third row shows an improvement if the 1st snake after the injection point has been retuned by mainly reducing the  $B_{out}$  setting to better match the incoming beam. The last two rows show that with the retuned RHIC snake, the Yellow beam would be rather insensitive to slight changes in the injection energy, whereas the Blue injection could be improved by a percent if the injection energy was lowered by  $\Delta G\gamma = 0.1$ .

Table 2 shows the effect of locating the partial snake at several other long straight sections in the AGS with the nominal settings for the RHIC snakes (i.e. a vertical stable

**TABLE 1.** Matching of  $\hat{n}_0$  into RHIC for various snake settings. The calculations are for a new snake in the AGS in the I20 straight section.

$G\gamma$	AGS Snake	Blue			Yellow		
		$\mu_1$	$\mu_2$	Match	$\mu_1$	$\mu_2$	Match
46.5	-20%	180°	180°	0.982	180°	180°	0.966
46.5	+20%	180°	180°	0.824	180°	180°	0.912
46.5	-20%	172°	180°	0.985	164°	180°	0.975
46.4	-20%	172°	180°	0.996	164°	180°	0.975
46.6	-20%	172°	180°	0.965	164°	180°	0.973

**TABLE 2.** Matching of  $\hat{n}_0$  into RHIC for different snake locations in the AGS. The last two rows show the matching with the present solenoidal snake located in the I10 straight section. Note that the injection septum and kicker are located in the L20 and A10 straight sections, respectively.

AGS Location	$G\gamma$	AGS Snake	Blue			Yellow		
			$\mu_1$	$\mu_2$	Match	$\mu_1$	$\mu_2$	Match
L10	46.5	+20%	180°	180°	0.985	180°	180°	0.987
L20	46.5	+20%	180°	180°	0.999	180°	180°	0.987
A10	46.5	+20%	180°	180°	0.998	180°	180°	0.980
A20	46.5	+20%	180°	180°	0.982	180°	180°	0.966
B10	46.5	+20%	180°	180°	0.955	180°	180°	0.949
I10	46.5	-5%	180°	180°	0.963	180°	180°	0.993
I10	46.5	+5%	180°	180°	0.923	180°	180°	0.974

spin direction). However for other partial snake strengths the matching might not be as good.

It is interesting to note that with the present solenoid snake in the AGS set to +5% at extraction, we would expect almost an 8% loss of polarization to the Blue with the partial snake field parallel to the beam. The last two rows of Table 2 show the spin injection efficiency for the present solenoidal partial snake. In fact in the 2002 polarized proton run the partial snake was parallel to the beam's direction, and we did observe a somewhat smaller polarization in the Blue ring than the Yellow ring. The efficiency for the Blue ring should be improved if we reverse the polarity of the partial snake in the next run.

## CONCLUSIONS

Even though the polarity of the partial snake in the AGS should not matter for acceleration, it becomes important when we consider the efficiency for matching the spin into the collider rings. The best solution for a 20% partial snake at I10 in the AGS would have the partial snake field antiparallel to the beam and one snake retuned for smaller spin rotation in each of the RHIC rings. In the Blue ring, the snake would only need to be retuned from 180° to 172° rotation to have a 99.6% transmission of polarization from

the AGS into the Blue ring. The Yellow ring would require a larger retuning of one snake to  $164^\circ$  of rotation; in this case the transmission would only be 97.5%. However tuning the snake to  $164^\circ$  would require a vertical realignment of the snake by about 0.5 cm to allow enough aperture for the orbit distortion in the snake at injection energy. Other solutions using one or two spin rotators may be possible without requiring a realignment of snakes; this will be explored in the future. Another more expensive solution with a snake in the W-line has previously been discussed in Reference [1].

## REFERENCES

1. I. Alekseev et al., *Design Manual Polarized Proton Collider at RHIC*, (1998).  
(<http://www.rhichome.bnl.gov/RHIC/Spin/design>)
2. T. Roser, "First Polarized Proton Collisions at RHIC", these proceedings (2003).
3. S. Y. Lee, *Spin Dynamics and Snakes in Synchrotrons*, World Scientific, Singapore (1997).
4. George Arfken, *Mathematical Methods for Physicists*, Academic Press, New York (1970).
5. W. MacKay and S. Peggs, "Accelerator Physics Coordinate Conventions", RHIC/AP/12 (1993).
6. M. J. Syphers, "Spin Motion through Helical Dipole Magnets", AGS/RHIC/SN No. 020, (1996).